



## Film dosimetry in water in a 23 MV therapeutic photon beam

L.J. van Battum\*, B.J.M. Heijmen

*Department of Clinical Physics, Dr. Daniel den Hoed Cancer Center, Postbus 5201, 3008 AE Rotterdam, The Netherlands*

Received 24 February 1994; revision received 6 December 1994; accepted 13 December 1994

### Abstract

The field size and water depth dependence of the measured optical density of Kodak XV-2 film, irradiated in a 23 MV photon beam has been investigated. The films were positioned in a water tank in a vertical plane containing the beam axis with the upper film edge parallel to the water surface at a depth of 0.3 mm. The observed field size and water depth dependence of the film sensitivity cannot be fully attributed to the usual variation of the photon spectrum with field size and water depth: measured optical densities do significantly depend on the amount of film material above the point of measurement and on the film orientation. A method for application of film for relative water dose measurements in a plane containing the beam axis in a 23 MV therapeutic photon beam is presented; the observed agreement between film and ionisation chamber measurements is very good: typically within 1% or 2 mm.

*Keywords:* Film dosimetry; Photon beams; Spectral sensitivity

### 1. Introduction

Film dosimetry of ionizing radiation has some important advantages over the widely applied thermoluminescent, semiconductor and ionometric techniques. Advantages are:

- (1) an enormous reduction in measuring time due to the simultaneous measurements for all points in the plane of the film;
- (2) a very high spatial resolution; and
- (3) the possibility of dose measurements in full planes in heterogeneously composed solid phantoms.

Mainly because of the first advantage, film dosimetry could be an interesting dosimetric method for measurements of the MM-50 Racetrack Microtron beams. This radiotherapy treatment unit, produced by the Swedish company Scanditronix and presently under installation in our institute, is equipped with computer controlled scanning electron and photon beams and a (dynamic) multi-leaf collimator, which can be used for production

of beams with non-flat profiles. Energies range from 10 to 50 MeV/MV.

Due to its advantages and its accuracy, film is now well established as a tool for high energy electron beam dosimetry in water, plastics and heterogeneously composed phantoms [1–3,5,8]. Film dosimetry in photon beams has been studied for energies ranging from  $^{60}\text{Co}$  to 45 MV [4–7,9,10] and many potential problems have been observed which are usually attributed to low energy scattered photons and the presence of high  $Z$  materials in the film emulsion.

Measured optical densities result from locally deposited film doses. Basically, in photon beams there are two mechanisms for deposition of energy in a film: (1) energy can be absorbed through direct interaction of a photon with the film, or (2) energy can be absorbed by energy deposition of a secondary electron, produced in an interaction of a photon with the medium surrounding the film, i.e. water in this study. Both the absolute and the relative contributions of mechanisms 1 and 2 depend on the local photon and secondary electron spectra and are therefore, in general, dependent on water depth and field size. For dosimetry, locally deposited water doses have to be determined; the film sensitivity is related to

\* Corresponding author.

the dose ratio  $D_{\text{film}}/D_{\text{water}}$  with  $D_{\text{film}}$  the dose delivered to the film in a point of measurement and  $D_{\text{water}}$  the dose delivered to water in the same point and under the same conditions, in case the film would not have been present. For dosimetry,  $D_{\text{film}}/D_{\text{water}}$  should ideally be independent of both field size and water depth.

The present study aims at the measurement of the sensitivity of films, positioned in a plane containing the beam axis, as a function of field size and water depth, and at the assessment of film orientation and disturbance effects. Moreover, a method for application of film for measurement of relative water dose distributions in a plane containing the beam axis has been developed and tested; relative water dose distributions determined with film have been compared with ionisation chamber measurements.

## 2. Materials

Kodak XV-2 X-ray films were irradiated in a Siemens KD-2 23 MV photon beam. The films were taken out of their ready pack and sealed in thin opaque polyethylene vacuumbags (Cronex Lo-Dose DuPont) with a thickness of 0.13 mm and maximum dimensions of  $25 \times 30 \text{ cm}^2$ . These opaque bags protect the films against water, environmental light and Cerenkov radiation.

A frame was used to position the sealed films exactly vertically in a water tank (Wellhöfer) with the upper film edge parallel to the water surface at a depth of approximately 0.3 mm (see Fig. 1). In this way, water surface perturbation due to surface tension effects was avoided. The distance of 0.3 mm between the film edge and the water surface was corrected for in the analysis of the films [1]. The films were positioned in a plane containing the beam axis, parallel to one of the sides of the square irradiation fields. The source-to-surface distance was 100 cm.

The films were processed in a standard automated Kodak RP X-Omat film processor. Quality assurance of the film processor was carried out with the X-Rite 380/381 densitometer/sensitometer system.

Processed films were digitized with a calibrated Wellhöfer WP 102 densitometer connected to a personal computer. The densitometer spotsize diameter was 2 mm. In-house developed software was used for scanning the films and for data analysis.

The net optical density is defined as the optical density measured by the densitometer, corrected for the background fog. The net optical density in a point of a processed film is related to the absorbed film dose, and was used in this study to assess the film sensitivity dependence on field size and water depth. In the remainder of this paper 'optical density' stands for 'net optical density'.

Ionometric measurements were performed in a

Wellhöfer water tank, using a thimble-type ionisation chamber with a diameter of 6 mm and a nominal volume of  $0.15 \text{ cm}^3$ . For percentage depth dose measurements the effective point of measurement of the chamber was taken at a fraction of 0.75 of the chamber radius in front of its centre. For the measurement of dose profiles no corrections were performed related with the finite size of the chamber.

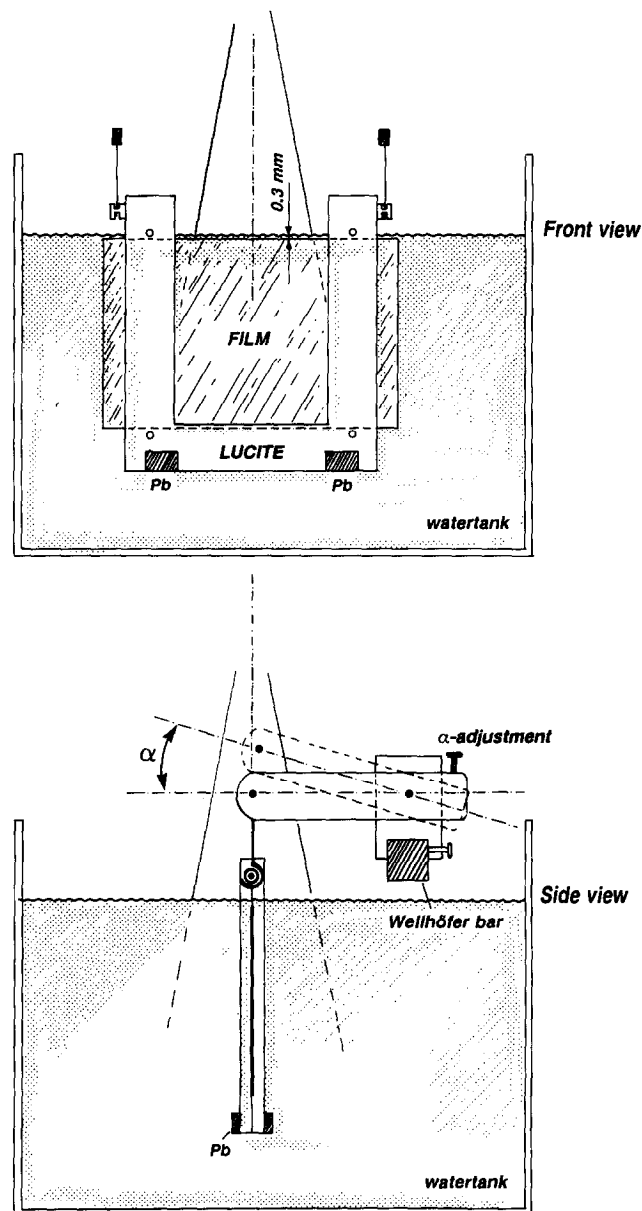


Fig. 1. The film positioning device applied in this study. Using the two  $\alpha$ -adjustment screws the upper film edge could be positioned exactly parallel to the water surface at a depth of 0.3 mm. This depth could be estimated using the Wellhöfer display, indicating the height of the bar in the water tank.

### 3. Methods

#### 3.1. Measurement of the film sensitivity dependence on field size and water depth

Films were irradiated for field sizes of  $4 \times 4 \text{ cm}^2$ ,  $10 \times 10 \text{ cm}^2$ ,  $20 \times 20 \text{ cm}^2$  and  $30 \times 30 \text{ cm}^2$ . For each field size, separate films were irradiated for the three water depths considered in this study: 5, 10 and 20 cm. For each field size and water depth combination the films were irradiated with a number of monitor units, such that always a fixed water dose of 50 cGy was delivered at the beam axis for the specified field size and water depth. The optical densities for the different field size and water depth combinations, measured at the beam axis at the specified water depth, were used for the assessment of the field size and water depth dependence of the film sensitivity; this implies that of each film only one data point was used.

Monitor units for delivery of 50 cGy were calculated using percentage depth dose curves and output factors measured in water with an ionisation chamber. The accuracy of the monitor unit calculation was better than 1%, i.e. for all field size and water depth combinations the difference with the  $10 \times 10/5$  combination (i.e. field size  $10 \times 10 \text{ cm}^2$ , water depth 5 cm) in delivered dose is estimated to be smaller than 1%.

Due to the limited resolution (1 MU) in the number of monitor units that can be selected at the treatment unit that was used, the actual depths of 50 cGy dose delivery differ slightly from the nominal depths of 5, 10 and 20 cm; actual depths were used in the analysis. Deviations from the nominal depths were always smaller than 0.5 cm.

Films were irradiated and processed in twelve sessions, i.e. on twelve different dates. In each session, measurements were performed for on the average five different field size and water depth combinations, always including the  $10 \times 10/5$  combination. For each combination involved in a particular session eight films were irradiated and the measured optical densities of these eight films were averaged and normalized to the average optical density for the eight films belonging to the  $10 \times 10/5$  combination, yielding the so-called normalized optical density for the particular field size and water depth combination. For all combinations, the determination of the normalized optical density was repeated in at least three sessions. The variation in the measured optical density of the eight films of a session belonging to a certain field size and water depth combination was typically, 0.7%, 1 relative SD. The average session-to-session variation in measured normalized optical densities was 1.3%, 1 relative SD. The total number of films used for this study was about 500.

It is well known that measured optical densities de-

pend on the film batch and the development conditions. Therefore, all films used in a session belonged to the same film batch. The films of each session were developed within a short overall period of time and in a consecutive order which was chosen to average out uncertainties in the results due to (potentially present) slow drifts in the film processor.

#### 3.2. Application of film dosimetry: determination of a sensitometric curve

Films, positioned vertically in a water tank as described in Section 2. and depicted in Fig. 1, were used for the measurement of relative water dose distributions. For the conversion of the optical density distributions of these films into water dose distributions, sensitometric curves were used describing the non-linear relationship between optical density and water dose [1].

For each dose distribution to be measured with film, several films (typically five) were irradiated under identical conditions. The five optical density distributions were converted into water dose distributions and averaged; based on a mutual comparison of these dose distributions, very strongly deviating films (cause unknown and rarely measured) were left out from the averaging process.

The films used for determination of relative water dose distributions and the films used for determination of the sensitometric curve were always from the same batch and irradiated and processed in the same measurement session.

#### Determination of a sensitometric curve

Sensitometric curves were derived from films irradiated in a  $10 \times 10 \text{ cm}^2$  open field, which were also positioned vertically in a water tank as described in Section 2 and depicted in Fig. 1. For each of these films the optical density distribution along the beam axis,  $OD(d)$ , was determined and the related absolute water dose distribution along the beam axis,  $D(d)$ , was calculated using the known depth dose curve for the  $10 \times 10 \text{ cm}^2$  field and the given number of monitor units;  $(OD(d), D(d))$  pairs were the points, constituting a sensitometric curve. Because of the relatively large dosimetric uncertainties in the build up region, data for  $d < d_{\text{max}}$  was not used for the production of sensitometric curves. To avoid systematic errors and to reduce the impact of statistical fluctuations several films were used for the production of a sensitometric curve, typically five. For noise reduction a polynomial function was fit to the  $(OD, D)$  points of a sensitometric curve, using the least squares method:

$$D(OD) = \sum_{n=1}^4 a_n \times OD^n$$

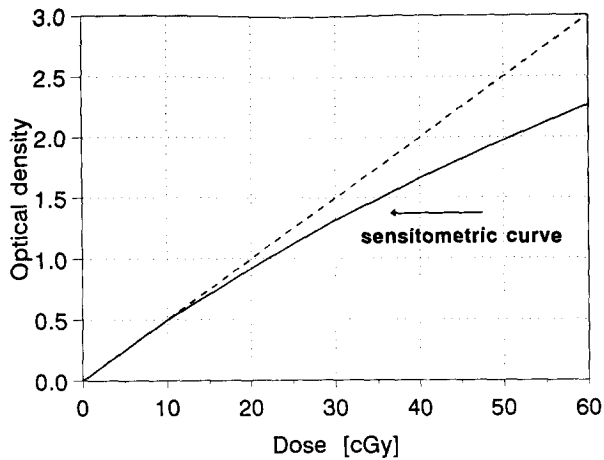


Fig. 2. The sensitometric curve used for the production of Figs. 4 and 5, derived from films irradiated in a  $10 \times 10 \text{ cm}^2$  field, using measured on-axis optical densities for water depths ranging from 5 cm to 20 cm.

with  $D(OD)$  the water dose corresponding to the optical density  $OD$ . Fig. 2 shows an example of a sensitometric curve that was determined using the method described above.

For film dosimetry in a plane containing the beam axis, the use of a sensitometric curve derived, as described above, from films positioned in the same plane, has several advantages. (1) Each film generates an array ( $OD(d), D(d)$ ) of data points for the sensitometric curve instead of a single point for horizontally positioned films. (2) For the open  $10 \times 10 \text{ cm}^2$  field a potentially existing depth dependence of the sensitivity of vertically

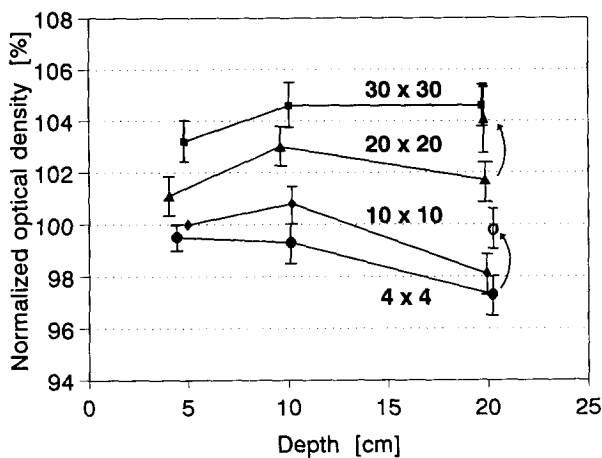


Fig. 3. The normalized optical density for a constant water dose of 50 cGy as a function of water depth and field size. The optical density for the  $10 \times 10 \text{ cm}^2$  field and a water depth of 5 cm was arbitrarily set to 100%. The height of each error bar is equal to two times the estimated standard deviation for the respective data point. For the open triangle and circle, see text.

positioned films can be calibrated into the sensitometric curve. As a consequence, at least for open fields not too much deviating from the  $10 \times 10 \text{ cm}^2$  field, conversion of optical densities into water doses yields an automatic correction for a water depth dependence of the film sensitivity.

The choice of the field size used for production of a sensitometric curve is essentially free. Therefore, for the measurement of dose distributions in very small or very large fields one could adapt the field size that is used for derivation of the sensitometric curve. Construction of a sensitometric curve as described above needs only a few films and the derivation of the curve from measured optical densities  $OD(d)$  along the beam axis can be fully automated. Therefore, one could also decide to construct separate sensitometric curves for small, intermediate and large fields. For this paper only the  $10 \times 10 \text{ cm}^2$  field was used for the production of sensitometric curves.

#### 4. Results and discussion

##### 4.1. The film sensitivity dependence on field size and water depth

The applied methods relevant for the results described in this paragraph are explained in Section 3.1.

In Fig. 3 the normalized optical densities for 5, 10 and 20 cm water depth are presented for the various field sizes; the error bars were calculated using observed fluctuations in measured optical densities (see Section 3.1). Fig. 3 demonstrates that the normalized optical density, related to a fixed water dose of 50 cGy, is dependent on the water depth and particularly on the field size; variations in film sensitivity of up to 8% were observed. Even

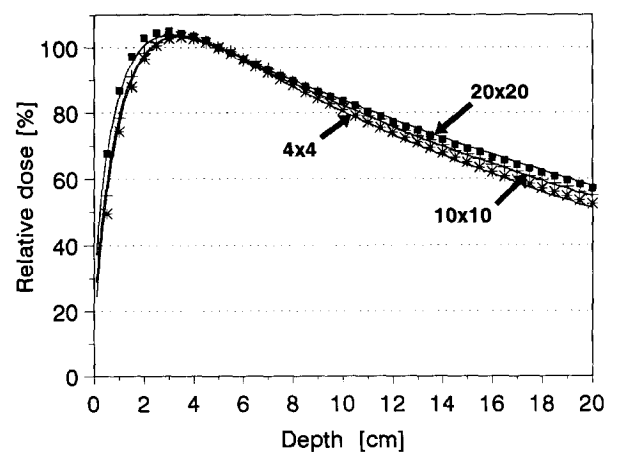


Fig. 4. PDD-curves measured with an ionisation chamber (markers) and with film (solid lines). For conversion of measured optical densities into relative doses the sensitometric curve depicted in Fig. 2 was used. All curves are normalized to 100% at 5 cm water depth.

at 5 cm water depth the optical density depends significantly on the field size: a  $30 \times 30 \text{ cm}^2$  field yielded a 3.8% higher optical density than a  $4 \times 4 \text{ cm}^2$  field yielded.

In order to investigate the influence of film orientation on this field size dependence, additional measurements were carried out with films positioned perpendicular to the beam axis at a water depth of 5 cm; for fields of  $4 \times 4$ ,  $10 \times 10$ ,  $20 \times 20$  and  $30 \times 30 \text{ cm}^2$  such films were exposed to a fixed water dose of 50 cGy. In contrast to the observed field size dependence of the measured optical density at 5 cm water depth for films irradiated parallel to the beam axis (see Fig. 3), no significant field size dependence was found for films irradiated perpendicular to the beam axis.

The observed decrease in film sensitivity at larger depths for the  $4 \times 4 \text{ cm}^2$  and the  $10 \times 10 \text{ cm}^2$  fields, shown in Fig. 3, is remarkable in comparison with observations reported in the literature [5,10]. Additional measurements were performed in order to investigate the influence of the presence of film material above the point of measurement on the observed decrease in measured optical density at larger depths: for the  $4 \times 4$  and  $20 \times 20 \text{ cm}^2$  fields, film strips were irradiated as explained in Fig. 1, but with the upper film edge positioned at a water depth of 15 cm, instead of the usual 0.3 mm. This means that no film material was present in the upper 15 cm of the water phantom. The film strips were exposed to a water dose of 50 cGy at the water depth of 20 cm. The measured optical density at 20 cm depth,

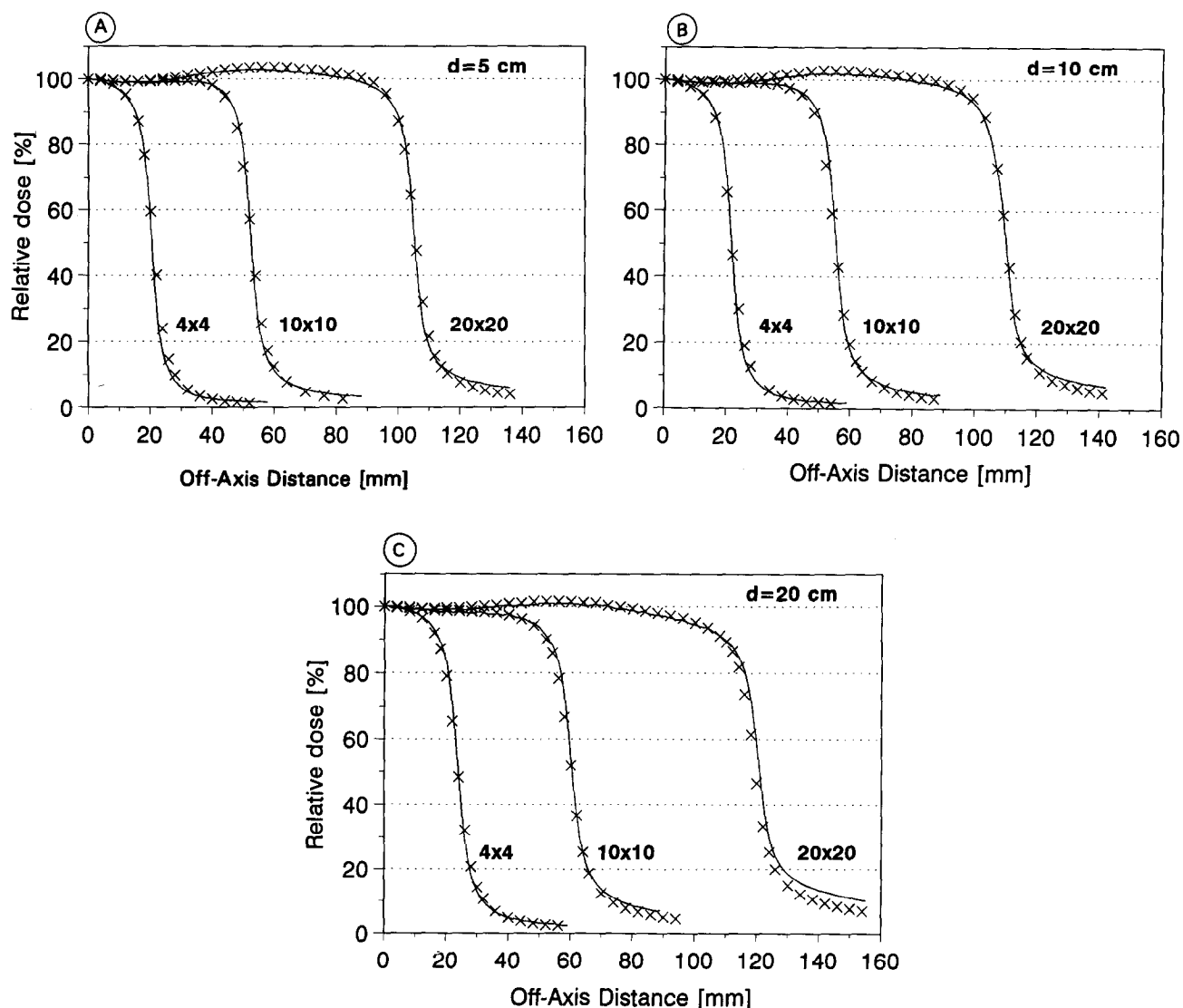


Fig. 5. Half profiles for square fields of  $4 \times 4$ ,  $10 \times 10$  and  $20 \times 20 \text{ cm}^2$  and water depths of 5, 10 and 20 cm, measured with ionisation chamber (crosses) and film (solid lines). The measured optical densities were converted to dose using the sensitometric curve depicted in Fig. 2.

normalized as usual to the  $10 \times 10/5$  combination, shows a significant increase with respect to the normalized density measured with the usual set-up, i.e. with film material present in the first 15 cm of the water tank: the open triangle and circle in Fig. 3 indicate the increased optical density (3%) due to the 15 cm reduction in film material between the water surface and the point of measurement at 20 cm water depth. The observed decrease in measured optical density at larger depths due to the presence of film material above the point of measurement can probably be attributed to an increased beam attenuation in film related with the density of film material which is higher than the water density [1].

If in Fig. 3 the curve for each field size would have been normalized to 'its own' measured optical density at 5 cm water depth (instead of on the density for the  $10 \times 10$  field at 5 cm depth), for each curve all points would have been within  $\pm 2\%$  equal to 100%, the largest deviations occurring at the larger depths. This limited

water depth dependence of the film sensitivity explains largely the good results described in the next section.

#### 4.2. Film dosimetry applied: examples

The applied methods relevant for the results described in this paragraph are explained in Section 3.2.

##### 4.2.1. Percentage depth dose (PDD) measurements

PDD curves for the  $4 \times 4$ ,  $10 \times 10$  and  $20 \times 20$  cm<sup>2</sup> fields, measured with an ionisation chamber and with film, are presented in Fig. 4. Fig. 2 shows the sensitometric curve that was used. All curves in Fig. 4 are normalized to 100% at a depth of 5 cm. The maximum deviation between the film-PDD curves and the ionisation chamber-PDD curves is 1% for the  $4 \times 4$  cm<sup>2</sup> field at a depth of 20 cm. When normalized at the depth of maximum dose, the maximum deviation between the film-PDD curves and the ionisation chamber-PDD

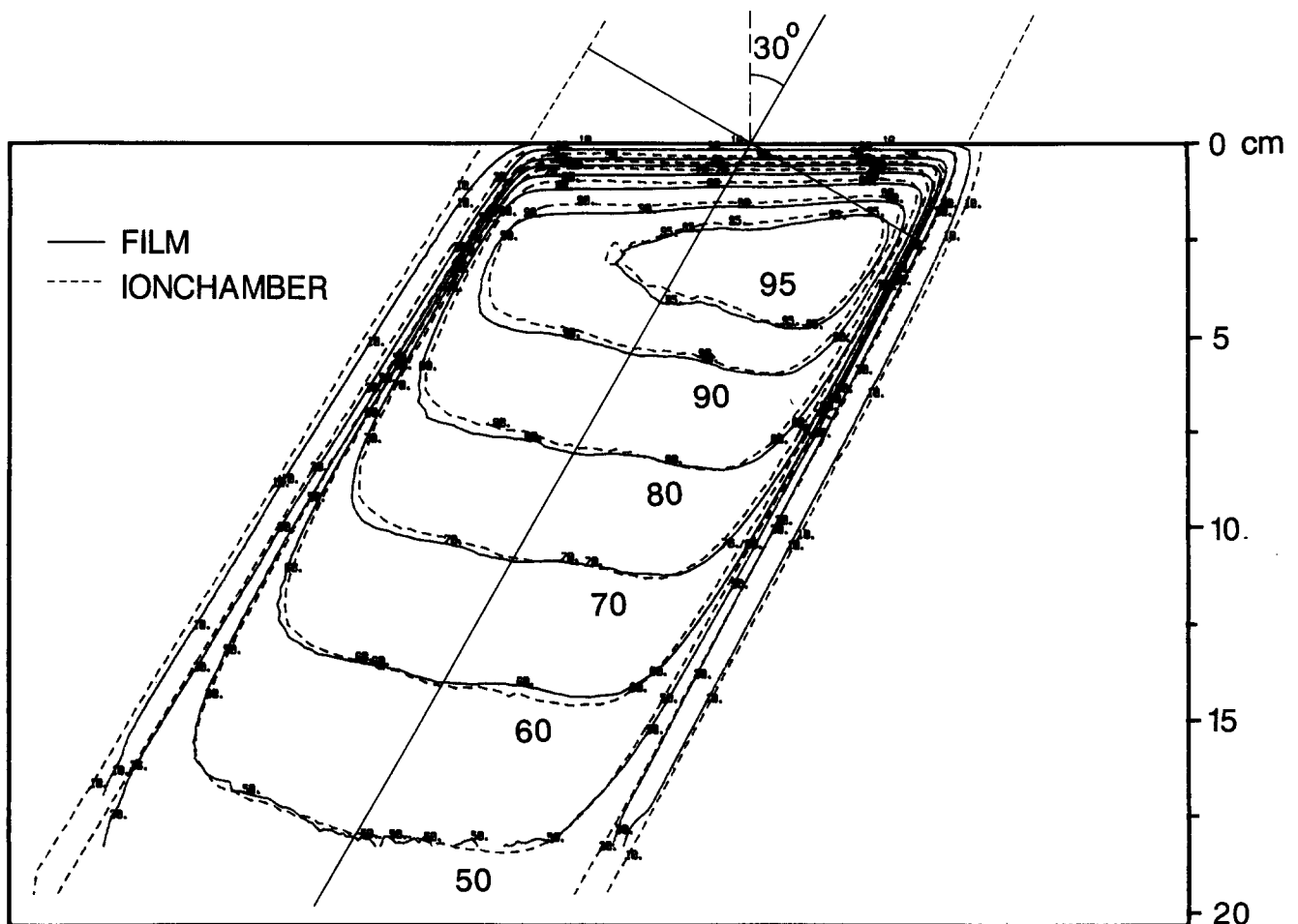


Fig. 6. Relative dose distributions measured with an ionisation chamber and with film for a field of  $10 \times 10$  cm<sup>2</sup> and an angle of incidence of  $30^\circ$ .

curves is 1.3% for the  $20 \times 20 \text{ cm}^2$  field at a depth of 20 cm.

In Fig. 4 the relative doses for the  $20 \times 20 \text{ cm}^2$  field around the depth of maximum dose, measured with film, are slightly lower than the ionisation chamber values. This deviation was observed for all field sizes larger than  $10 \times 10 \text{ cm}^2$ .

#### 4.2.2. Dose profile measurements

Off-axis photon spectra are known to differ from the spectrum on the beam axis, especially in the penumbra region. This effect could influence the accuracy of dose profiles measured with film. In Fig. 5 profiles are presented, measured with the ionisation chamber and with film. Profiles are plotted for depths of 5, 10 and 20 cm and fields of  $4 \times 4$ ,  $10 \times 10$  and  $20 \times 20 \text{ cm}^2$ ; all profiles are normalised to 100% at the beam axis. Fig. 5 shows a good overall agreement between ionisation chamber measurements and film measurements. Small differences occur in the steepness of the penumbra and for points situated beyond the geometrical field edge. The penumbra measured with film is generally somewhat steeper than the ionisation chamber penumbra; for the nine cases presented in Fig. 5 the average difference between ionisation chamber and film in the 20–80% penumbra width is  $1.5 \pm 0.5 \text{ mm}$  (1 SD). This difference in penumbra width is due to the finite diameter of the ionisation chamber [6]. The overshoot in relative dose measured with film for points situated more than 1 cm beyond the geometrical field edge is probably due to the relatively large amount of low energy scattered photons in this region. The results inside the geometrical field edges indicate a film sensitivity dependence on off-axis position, typically smaller than 1%.

Fig. 6 shows film and ionisation chamber dose distributions for a  $10 \times 10 \text{ cm}^2$  field and an angle of incidence of 30 degrees. The sensitometric curve was determined for the open  $10 \times 10 \text{ cm}^2$  field with perpendicular incidence, as described in Section 3.2. Excellent agreement between film and ionisation chamber measurements was found: the relative dose distributions agree generally within 1% or 2 mm. Similar results were found for wedge fields.

## 5. Conclusions

The application of film dosimetry in water in a 23 MV photon beam has been investigated. The films were positioned in a vertical plane containing the beam axis with the upper film edge parallel to the water surface at a depth of 0.3 mm.

For films positioned in a plane containing the beam axis, the film sensitivity depends significantly on the water depth and especially on the field size; for a fixed water dose, variations in measured optical density of up

to 8% have been observed. For each individual field size studied, the water depth dependence of the film sensitivity is always within 2%. Inside the geometrical field edges the film sensitivity dependence on off-axis position is typically within 1% for field sizes of  $4 \times 4$  to  $20 \times 20 \text{ cm}^2$  and water depths of 5–20 cm.

For films positioned perpendicularly to the beam axis at 5 cm water depth no field size dependence of the film sensitivity has been found, in contrast to the observed field size dependence at this depth for films positioned parallel to the beam axis. Moreover, for films positioned parallel to the beam axis a significant reduction in film sensitivity at larger water depths has been observed which has been attributed to the presence of film material above the point of measurement. Therefore, the observed field size and water depth dependence of the sensitivity of films positioned parallel to the beam axis cannot be fully attributed to the well known variation in photon spectrum with water depth and field size.

A method for application of film for measurement of relative water dose distributions in a plane containing the beam axis has been developed and tested. Relative water dose distributions derived from films were compared with ionometrically determined dose distributions; the agreement was generally within 1% or 2 mm. To obtain such a good agreement, dose distributions of several films were averaged, leaving out strongly deviating films. We recommend to measure at least three films per set-up.

## Acknowledgements

The authors are indebted to B. Göbel and E.A. Loeff for their assistance during measurements, to B.A. v.d. Leije for the production of software and to M.L.P. Dirx, H. Huizenga, J.A. v.d. Poel, J.P.C. van Santvoort and A.G. Visser for valuable discussions and for comments on the manuscript.

## References

- [1] Battum, L.J. van and Huizenga, H. Film dosimetry of clinical electron beams. *Int. J. Radiat. Oncol., Biol. Phys.* 18: 69–76, 1990.
- [2] Dutreix, J. and Dutreix, A. Film dosimetry of high energy electrons. *Ann. N.Y. Acad. Sci.* 161: 33–43, 1969.
- [3] El-Khatib, E., Antolak, J. and Scrimger, J. Evaluation of film and thermoluminescent dosimetry of high-energy electron beams in heterogeneous phantoms. *Med. Phys.* 19(2): 317–323, 1992.
- [4] Evans, M.D.C. and Schreiner, L.J. A simple technique for film dosimetry. *Radiother. Oncol.* 23: 265–267, 1992.
- [5] Johansson, K.A. Studies of Different Methods of Absorbed Dose Determination and a Dosimetric Intercomparison at the Nordic Radiotherapy Centres. PhD Thesis, 1982.
- [6] Metcalfe, P., Kron, T., Elliott, A., Wong, T. and Hoban, P. Dosimetry of 6 MV X-ray beam penumbra. *Med. Phys.* 20(5): 1439–1445, 1993.

- [7] Muench, P.J., Meigooni, A.S., Nath, R. and McLaughlin, W.L. Photon energy dependence of the sensitivity of radiochromic film and comparison with silver halide film and LiF TLDs used for brachytherapy dosimetry. *Med. Phys.* 18(4): 769–775, 1991.
- [8] Shiu, A.S., Otte, V.A. and Hogstrom, K.R. Measurement of dose distributions using film in therapeutic electron beams. *Med. Phys.* 16(6): 911–915, 1989.
- [9] Stern, R.L., Fraass, B.A., Gerhardsson, A. and McShan, D.L. Generation and use of measurement-based 3-D dose distributions for 3-D dose calculation verification. *Med. Phys.* 19(1): 165–173, 1992.
- [10] Williamson, J.F., Khan, F.M. and Sharma, S.C. Film dosimetry of megavoltage photon beams: a practical method of isodensity-to-isodose curve conversion. *Med. Phys.* 8(1): 94–98, 1981.